matic rings and hyperconjugation with alkyl groups. Because conjugation and hyperconjugation are much weaker for Si than for C (Si=C versus C=C), such effects do not provide the restoring forces to maintain planarity around Si that are present in C systems. These effects have been previously recognized in silyl radicals. Whereas carbon radicals tend to be planar, analogous silyl radicals are nonplanar: for example, $Me_3Si\cdot$ has an out-of-plane angle of about 15° (*18*). In the same manner, the silyl cation herein easily distorts from the plane to relieve external sources of strain. This distortion explains why the ^{29}Si NMR chemical shift (δ = 92.3 in benzene) moves ~90 parts per million (ppm) (*12*) from the position of the hydride (δ = 0.2) rather than the 300 ppm or so expected for a planar structure (*8*). Chemical shift is extremely sensitive to such geometrical distortions. It is possible that the use of π-conjugating or more bulky substituents could bring the geometry around Si closer to planarity. This structure, albeit nonplanar, is best termed a stable silyl cation because it entirely lacks coordination to the anion, the distance to the weakly coordinating toluene is unprecedented for bonding, and the toluene lacks any of the geometric characteristics of a σ complex.

REFERENCES AND NOTES

1. F. C. Whitmore, L. H. Sommer, J. Gold, *J. Am. Chem. Soc.* **69**, 1976 (1947); F. P. Price, *ibid.* **70**, 871 (1948); C. G. Swain, R. M. Esteve, Jr., R. H. Jones, *ibid.* **71**, 965 (1949).
2. Y. Apeioig and P. v. R. Schleyer, *Tetrahedron Lett.* **1977**, 4647 (1977); S. A. Godleski, D. J. Heacock, J. M. McKelvey, *ibid.* **23**, 4453 (1982); T. Truong, M. S. Gordon, P. Boudjouk, *Organometallics* **3**, 484 (1984).
3. B. G. Hobrock and R. W. Kiser, *J. Phys. Chem.* **66**, 155 (1962); W. P. Weber, R. A. Felix, A. K. Willard, *Tetrahedron Lett.* **1970**, 907 (1970); M. K. Murphy and J. L. Beauchamp, *J. Am. Chem. Soc.* **99**, 2085 (1977); W. J. Pietro and W. J. Hehre, *ibid.* **104**, 4329 (1982).
4. Y. Apeloig and A. Stanger, *J. Am. Chem. Soc.* **109**, 272 (1987); H. Mayr, N. Basso, G. Hagen, *ibid.* **114**, 3060 (1992).
5. For a review, see R. J. P. Corriu and M. Henner, *J. Organomet. Chem.* **74**, 1 (1974).
6. P. D. Lickiss, *J. Chem. Soc. Dalton Trans.* **1992**, 1333 (1992).
7. J. B. Lambert, W. J. Schulz, Jr., J. A. McConnell, W. Schilf, *J. Am. Chem. Soc.* **110**, 2201 (1988); J. B. Lambert, L. Kania, W. Schilf, J. A. McConnell, *Organometallics* **10**, 2578 (1991).
8. G. A. Olah, L. Heiliger, X.-Y. Li, G. K. S. Prakash, *J. Am. Chem. Soc.* **112**, 5991 (1990).
9. G. K. S. Prakash *et al.*, *ibid.* **109**, 5123 (1987).
10. M. Kira, T. Hino, H. Sakurai, *ibid.* **114**, 6697 (1992).
11. X. Yang, C. L. Stern, T. J. Marks, *Organometallics* **10**, 840 (1991); J. C. W. Chien, W.-M. Tsai, M. D. Rausch, *J. Am. Chem. Soc.* **113**, 8570 (1991).
12. J. B. Lambert and S. Zhang, *Chem. Commun.* **1993**, 383 (1993).
13. A colorless, prismatic crystal (approximate dimensions, 0.26 mm by 0.48 mm by 0.14 mm) was mounted on a glass fiber. All measurements were made on an Enraf-Nonius CAD-4 diffractometer with graphite monochromated Mo Kα radiation. Cell constants and an orientation matrix for data collection corresponded to a triclinic cell with a = 13.168(4) Å, b = 17.593(3) Å, c = 18.117(4) Å, V = 4131(3) Å^3, α = 86.19(2)°, β = 84.21(2)°, and γ = 82.24(2)°, where the number in parentheses is the error in the last digit. For number of molecules in the unit cell Z = 4 and formula weight = 974.56, the calculated density is 1.567 g cm^{-3}. Data were collected at −120° ± 1°C with the ω-θ scan technique to a maximum 2θ value of 48.0°. From 4627 observed reflections, the structure was solved by direct methods (SHELXS-86) in the space group $P\bar{1}$. The unit cell contained four molecules of Et_3Si^+ $(C_6F_5)_4B^-$ (two of which were crystallographically distinct from the other two) and eight molecules of the solvent, toluene. Only silicon and fluorene were refined anisotropically. Hydrogen atoms were included as fixed contributors at calculated positions, except for the hydrogen on the para carbon of the toluene closer to Si. The final cycle of full-matrix, least squares refinement led to unweighted and weighted agreement factors of R = 0.069 and R_w = 0.666. All calculations were done with TEXSAN software.
14. K. Hensen, T. Zengerly, P. Pickel, G. Klebe, *Angew. Chem. Int. Ed. Engl.* **22**, 725 (1983).
15. Z. Xie *et al.*, *Chem. Commun.* **1993**, 384 (1993).
16. F. Effenberger *et al.*, *J. Am. Chem. Soc.* **109**, 882 (1987).
17. W. S. Sheldrick, in *The Chemistry of Organic Silicon Compounds*, S. Patai and Z. Rappoport, Eds. (Wiley, Chichester, U.K., 1989), p. 246.
18. F. K. Cartledge and R. V. Piccione, *Organometallics* **3**, 299 (1984); I. Carmichael, *J. Phys. Chem.* **89**, 4727 (1985).

19. Supported by NSF grant CHE-8910841.

10 March 1993; accepted 26 April 1993

Optically Active Carbon: Kinetic Resolution of C_{76} by Asymmetric Osmylation

Joel M. Hawkins* and Axel Meyer

The chiral fullerene C_{76} was kinetically resolved by asymmetric osmylation providing an example of an optically active allotrope of a pure element. C_{76} recovered from the treatment of racemic C_{76} with OsO_4 and a chiral alkaloid ligand, showed a specific rotation $[\alpha]_D$ of −4000° (>97 percent enantiomeric excess) and a circular dichroism spectrum corresponding to the ultraviolet spectrum. Regenerated C_{76} formed by reducing the asymmetrically osmylated C_{76} with $SnCl_2$ was enriched in the opposite enantiomer. Analysis of the local curvature of the C_{76} molecule indicated that OsO_4 should selectively add to 2 of the 30 types of bonds in C_{76}. This regioselectivity was supported chromatographically and interpreted in terms of the kinetic resolution.

The double-helical fullerene C_{76} has been described as "one of the most fascinating molecular architectures ever seen in nature" (*1*). This chiral allotrope of carbon has been isolated in racemic form as a minor component of Krätschmer-Huffman soot (*1*, *2*). Numerous attempts to resolve C_{76} into its enantiomers by classical means have not been successful. Here we report the kinetic resolution of C_{76} by asymmetric osmylation whereby the enantiomers of C_{76} are discriminated chemically, producing an optically active sample of elemental carbon.

We have shown that fullerene osmylation is selective with respect to stoichiometry (*3*, *4*), regiochemistry (*5*–*7*), and stereochemistry (*8*). The kinetic resolution of C_{76} combines all of these attributes, one enantiomer of the substrate reacting faster with an asymmetric reagent than the other enantiomer. The starting material becomes enriched in the less reactive enantiomer, and the reaction product corresponds to the more reactive enantiomer (*9*). We have shown that Sharpless' cinchona alkaloid-derived ligands for the asymmetric dihydroxylation of olefins (*10*, *11*) can be used for the asymmetric bisosmylation of C_{60} giving chiral $C_{60}(OsO_4py_2)_2$ isomers with optical rotations up to 3700° (*8*). A potential difficulty with C_{76} is one of regiochemistry, C_{76} contains 30 types of carbon-carbon bonds, and reaction at different bonds could give different enantiomer discriminations which might oppose each other. Considering that C_{76} is most likely to osmylate at the fusion of two six-membered rings, as found for C_{60} (*5*, *6*), this still

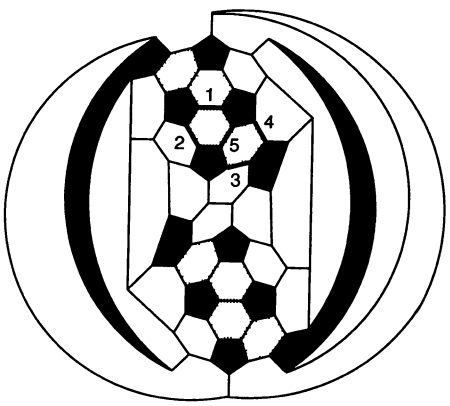

Fig. 1. Representation of C_{76} showing the five symmetry-independent pyracylene-type carbon-carbon bonds (bold bonds numbered 1 to 5) which combine to give reactive chrysene-shaped units (shaded). Five-membered rings are blackened.

Department of Chemistry, University of California, Berkeley, CA 94720.

*To whom correspondence should be addressed.

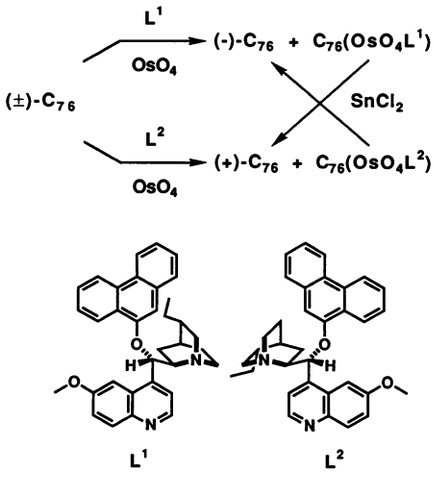

Scheme 1. Kinetic resolution of C_{76} by asymmetric osmylation in the presence of chiral ligands $\mathbf{L^1}$ and $\mathbf{L^2}$. Recovered and regenerated C_{76} are enriched in opposite enantiomers. Pseudoenantiomers $\mathbf{L^1}$ and $\mathbf{L^2}$ give opposite enantiomers of C_{76}.

leaves 15 types of six-membered ring fusions as potential reaction sites.

Our results with C_{70} suggested that C_{76} may osmylate with some regioselectivity as required for effective kinetic resolution. Addition of OsO_4 to C_{70} occurs selectively at pyracylene-type positions within the corannulene apex (major isomer) and at the edge of the corannulene apex (minor isomer) (*7*). Osmylation occurs mainly at the most distorted bonds (with the greatest local curvature) rather than at the shortest bonds, with the greatest bond order. C_{76} contains five distinct pyracylene-type carbon-carbon bonds which repeat to form chrysene-shaped units (Fig. 1). An analysis of an ab initio calculated structure of C_{76} (*12*) with the program POAV1 (*13*) showed that two of these bonds are particularly distorted (Fig. 2). Bonds 1 and 5 at the six-membered ring fusions within the reactive chrysene units involve carbon atoms which are pyramidalized more than those in the most reactive site of C_{70} (σ-π

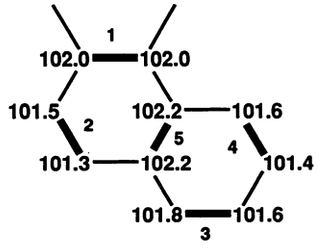

Fig. 2. Five symmetry-independent pyracylene-type carbon-carbon bonds (bold bonds numbered 1 to 5) that constitute the reactive chrysene-shaped units of C_{76}. Carbon atoms are labeled with their σ-π interorbital angles indicating their degree of pyramidalization.

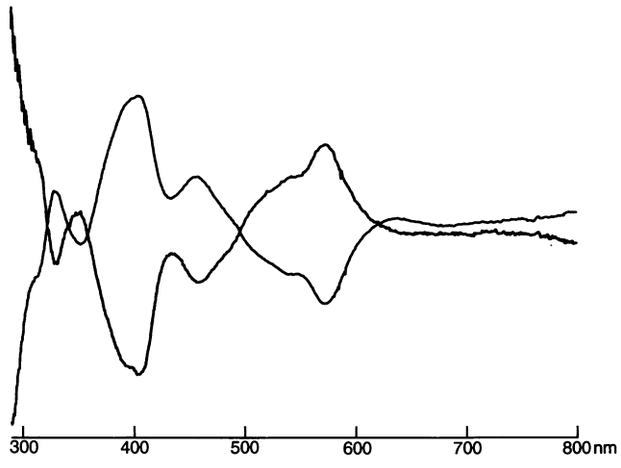

Fig. 3. Circular dichroism spectra of carbon: CD spectrum (290 to 800 nm) of kinetically resolved C_{76} (from $\mathbf{L^1}$) after 95% conversion (negative at 573 nm) superimposed on the CD spectrum of regenerated C_{76} after 33% conversion (positive at 573 nm). Kinetically resolved C_{76} [38 × 10^{-6} M in toluene, wavelength in nanometers, and $\Delta\epsilon$ (in parentheses) in liters per mole per centimeter]: 315 (sh, −11.7), 330 (+8.91), 354 (−4.25), 394 (sh, +29.4), 405 (+31.6), 460 (+12.6), 541 (sh, −11.1), 573 (−18.2), 639 (+2.55).

interorbital angles ≥102.0°, compared to 102.0 and 101.9° within the corannulene apex of C_{70} (*14*). If C_{76} behaves like C_{70} and preferentially reacts at sites of greatest local curvature, then osmylation should give two major isomers of $C_{76}(OsO_4L_2)$ corresponding to bonds 1 and 5. Subsequent high-performance liquid chromatography (HPLC) analysis of $C_{76}(OsO_4py_2)$ under conditions that cleanly separate the isomers of $C_{70}(OsO_4py_2)$ (*7*) showed two major peaks.

We isolated pure C_{76} from fullerene extract by two successive gravity column chromatographies on neutral alumina (15 and 20% toluene in hexane) followed by HPLC on a Regis Buckyclutcher I column (50% toluene in hexane). Four chiral ligands that seemed the most appropriate from our asymmetric bisosmylations of C_{60} were screened for the kinetic resolution of C_{76} (Scheme 1). Treatment of 350-μg (*15*) samples of pure C_{76} with one equivalent of OsO_4 and an excess of chiral ligand in toluene at 0°C was followed by chromatographic separation of unreacted C_{76} from osmylated C_{76} [silica gel, toluene to elute C_{76}, 5% 4-*tert*-butylpyridine in $CHCl_3$ to elute $C_{76}(OsO_4L_2)_n$]. In order to compare recovered starting material and product stereochemistries, it was necessary to convert osmylated C_{76} back into C_{76}. We explored various reducing agents with osmylated C_{60} as a model and found that C_{60} could be quantitatively regenerated from $C_{60}(OsO_4py_2)$ by treatment with $SnCl_2$ in pyridine (Eq. 1). This technique was applied to the present experiments.

$$C_{60}(OsO_4py_2) \xrightarrow[\text{Pyridine, 25°C}]{\text{Excess } SnCl_2} C_{60}\ (100\%) \quad (1)$$

The recovered starting materials, C_{76}, and products (C_{76} from the reduction of $C_{76}(OsO_4py_2)_n$) showed significant optical activity and well-defined circular dichroism (CD) spectra. Phenanthrene-containing chiral ligands were found to be the best for these experiments. Pseudoenantiomers $\mathbf{L^1}$ and $\mathbf{L^2}$ gave enantiomers of recovered C_{76} (as expected based on Sharpless' chemistry) (*10*, *11*), and unreacted (starting material) and regenerated (product) C_{76} were enriched in opposite enantiomers (as expected for a kinetic resolution), (see Scheme 1). A 2.7-mg sample of C_{76} was treated with 0.9 equivalents of OsO_4 and 5 equivalents of $\mathbf{L^1}$, and the starting material and products were analyzed after 33% conversion. The recovered starting material was resubjected to the osmylation conditions bringing the total conversion up to 95%. Figure 3 shows the CD spectrum of recovered C_{76} after 95% conversion superimposed on the CD spectrum of regenerated C_{76} after 33% conversion. The mirror image spectra correspond to mirror image molecules. The CD

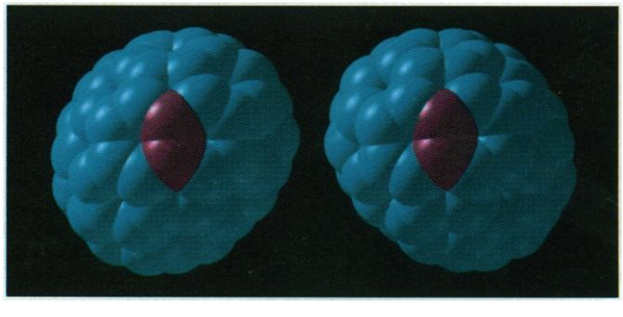

Fig. 4. Enantiomers of C_{76} viewed above the most distorted bond (bond 5, purple) showing how the van der Waals surfaces curve away from the probable main reaction site with pronounced handedness. [Surfaces generated from ab initio coordinates (*13*).]

peaks at 330, 354, 405, 460, and 573 nm clearly correspond to the ultraviolet peaks of C_{76} at 329, 354 (sh), 405, 452 (sh), and 574 nm (*16*), establishing that the CD spectra correspond to resolved C_{76}. The kinetically resolved C_{76} after 95% conversion showed an optical rotation $[\alpha]_D$ of −4000° (concentration: 0.0034, in toluene). The starting material analyzed after 33% conversion showed 28% of this optical activity. These two points in the relationship between optical activity and conversion in the kinetic resolution allowed calculation of the enantiomeric excess of the recovered starting material (*17*); the recovered C_{76} after 95% conversion is >97% enantiomeric excess. The maximum specific rotation of C_{76} is estimated to be 4000 ± 400° at the sodium *D*-line, a value comparable with the helicenes (*18*).

The differences between the enantiomers of C_{76} are not immediately obvious from molecular models. However, when you constrain your view to a particular type of bond, such as the site of greatest local curvature (bond 5), the differences become clearer (Fig. 4). This exercise has implications at the molecular level. Resolution techniques which interact with C_{76} molecules over their entire surface, such as chiral stationary-phase HPLC, manifest little difference between the enantiomers and ineffective resolution. However, resolution techniques which selectively operate upon a particular part of C_{76}, such as regioselective asymmetric osmylation, have a much better chance of enantiomer discrimination. For example, the approach to bond 5 in Fig. 4 shows that the van der Waals surface curves away from this probable main reaction site with very different handedness for the two enantiomers. Chiral recognition may involve diastereotopic attractive π-π interactions between the phenanthryl units of L^1 and L^2 and these contoured fullerene surfaces (*19*, *20*). This technology could be applied to the resolution of other chiral fullerenes.

REFERENCES AND NOTES

1. R. Ettl, I. Chao, F. Diederich, R. L. Whetten, *Nature* **353**, 149 (1991).
2. F. Diederich and R. L. Whetten, *Acc. Chem. Res.* **25**, 119 (1992).
3. J. M. Hawkins, A. Meyer, T. A. Lewis, S. Loren, F. J. Hollander, *Science* **252**, 312 (1991).
4. J. M. Hawkins, *Acc. Chem. Res.* **25**, 150 (1992).
5. ———, S. Loren, A. Meyer, R. Nunlist, *J. Am. Chem. Soc.* **113**, 7770 (1991).
6. J. M. Hawkins *et al.*, *ibid.* **114**, 7954 (1992).
7. J. M. Hawkins, A. Meyer, M. A. Solow, unpublished results.
8. J. M. Hawkins, A. Meyer, M. Nambu, in preparation.
9. For example, see V. S. Martin *et al.*, *J. Am. Chem. Soc.* **103**, 6237 (1981).
10. K. B. Sharpless *et al.*, *J. Org. Chem.* **56**, 4585 (1991).
11. K. B. Sharpless *et al.*, *ibid.* **57**, 2768 (1992).
12. J. R. Colt and G. E. Scuseria, *J. Phys. Chem.* **96**, 10265 (1992).
13. R. C. Haddon, *Acc. Chem. Res.* **21**, 243 (1988).
14. As with C_{70}, the bonds between the most pyramidalized carbons in C_{76} are not the shortest bonds.
15. Small quantities of C_{76} were measured spectrophotometrically.
16. The UV spectrum of C_{76} in toluene is similar to the published spectrum in CH_2Cl_2 (*1*). The shoulder at 452 nm in CH_2Cl_2 is not well defined in toluene, so the value from CH_2Cl_2 is listed.
17. A. R. Schoofs and J.-P. Guetté, in *Asymmetric Synthesis*, J. D. Morrison, Ed. (Academic Press, New York, 1983), vol. 1, chap. 3.
18. K. P. Meurer and F. Vögtle, in *Topics in Current Chemistry*, F. L. Boschke, Ed. (Springer-Verlag, New York, 1985), vol. 127, pp. 32–53.
19. Chiral recognition in the asymmetric bisosmylation of C_{60} appears to be governed by attractive interactions (*8*).
20. Regeneration of C_{76} separately from the two major isomers of $C_{76}(OsO_4py_2)$ will indicate whether the chiral recognition mechanisms for the two major reaction paths are additive or partially subtractive.

21. We thank N. Holden for a generous loan of fullerene extract, G. Scuseria for his calculated coordinates of C_{76}, R. Haddon for a copy of his POAV analysis program, S. Loren and T. Robinson for computer expertise, Regis Chemical Company for a complementary Buckyclutcher I column, and K. B. Sharpless for chiral ligand samples. J.M.H. is grateful to NSF (Presidential Young Investigator Award, CHE-8857453), DOE, the Camille and Henry Dreyfus Foundation (Teacher-Scholar Award), Merck Sharp & Dohme Research Laboratories, the Shell Oil Company Foundation, Xerox Corporation, Monsanto Company, Hoffmann-La Roche Inc., Chevron Research and Technology Company, and Eli Lilly and Company for financial support.

30 March 1993; accepted 5 May 1993

Evidence from Western North America for Rapid Shifts in Climate During the Last Glacial Maximum

Bruce D. Allen and Roger Y. Anderson

The Estancia basin in southwestern United States contains evidence for strong and rapid pulsations in the supply of moisture brought into the region during the last ice age. The pulses were recorded during episodes of stream discharge that spread plumes of fresh water laden with quartz sand over the saline lake. The largest pulses in stream discharge lasted only a few decades, were organized into cycles that were spaced approximately 200 to 250 and 2000 years apart, and were of sufficient magnitude to freshen and maintain the lake at its maximum recorded elevation.

When the last great ice sheet was nearing collapse, high-latitude regions may have warmed by as much as 7°C within 40 to 50 years (*1*). In Greenland, the quantity of dust trapped in ice and the isotopic composition of the ice changed dramatically in less than 20 years (*1*, *2*). Evidence for rapid shifts in climate comes from sites above 65°N, and little is known about sudden changes in climate in the region that lies to the south of the Laurentide ice sheet. In this report we describe evidence for large and equally rapid changes in precipitation from pluvial Lake Estancia, central New Mexico, 35°N, 106°W (Fig. 1A).

Today, the floor of Estancia basin is occupied by numerous playas. During the last glacial maximum and deglaciation, a greatly expanded Lake Estancia experienced two major highstands, one beginning ~19,700 years ago and another ~13,700 years ago (Table 1). The early highstand formed the highest shoreline at 1890 m, at which time the lake had a surface area of 1100 km^2 and a water depth of 45 m. The high ratio of lake surface area to drainage area (Fig. 1B) produced large fluctuations in water volume and hydrochemistry as a result of changes in precipitation and evaporation. The absence of glaciers in the upland drainage means that recharge was entirely from precipitation, direct runoff, and ground water, with no lag effects from melting ice.

The fauna preserved in Estancia sediment consists largely of calcareous valves of ostracodes. Two species, *Limnocythere staplini* and *Candona rawsoni*, are present throughout most of the lake sequence. Other species, including *Cytherissa lacustris*, *Candona caudata*, and *Limnocythere ceriotuberosa*, are restricted to narrow stratigraphic zones throughout the central area of the basin and were used to correlate between localities.

By tracing lowstand strata to their shoreline elevation, we determined that groundwater discharge had maintained a minimum pool of ~400 km^2 throughout the period of deglaciation until ~12,000 years ago. The continuity of centimeter-scale layers of sediment and faunal zones over distances of several kilometers in the area once covered by the permanent pool indicates that accumulation was continuous and that the basin contains an uninterrupted record of climate variability.

Age control for changes within the glacial maximum highstand (gmh) sequence (~20,000 to ~15,000 years ago) is provided by radiocarbon dates of various organic

Department of Earth and Planetary Sciences, University of New Mexico, Albuquerque, NM 87131.